SIMULATION OF PLASMA TRANSPORT IN THE SCRAPE-OFF REGION OF ASDEX

G. Becker, C.E. Singer+)

IPP III/75 November 1981

MAX-PLANCK-INSTITUT FÜR PLASMAPHYSIK

8046 GARCHING BEI MÜNCHEN

MAX-PLANCK-INSTITUT FÜR PLASMAPHYSIK

GARCHING BEI MÜNCHEN

SIMULATION OF PLASMA TRANSPORT IN THE
SCRAPE-OFF REGION OF ASDEX

G. Becker, C.E. Singer+)

IPP III/75 November 1981

+) Princeton Plasma Physics Laboratory

Die nachstehende Arbeit wurde im Rahmen des Vertrages zwischen dem Max-Planck-Institut für Plasmaphysik und der Europäischen Atomgemeinschaft über die Zusammenarbeit auf dem Gebiete der Plasmaphysik durchgeführt.

IPP III/75 G. Becker
C.E. Singer

SIMULATION OF PLASMA TRANSPORT IN THE SCRAPE-OFF REGION OF ASDEX

November 1981
(in English)

ABSTRACT

Ohmically heated diverted discharges in ASDEX are simulated by a one-dimensional self-consistent scrape-off model in the BALDUR transport code. The model includes anomalous cross-field diffusivities ($D_\perp$, $\chi_{e\perp}$) and convective particle losses $\| \vec{B}$ ($n\, v_\Gamma$) and separately treats the losses due to heat conduction and convection along the magnetic field. A best fit to the experiments is obtained with a subsonic flow velocity $v_\Gamma = 1/7\ v_s$, a recycling coefficient $\rho = 0.2$ and $D_\perp = 1.6 \times 10^3\ cm^2\ s^{-1}$. The anomalously high $D_\perp$ and $\chi_{e\perp}$ values required in the scrape-off zone do not differ much from the transport coefficients in the bulk plasma. Computed scrape-off scale-heights for the density are independent of ρ since the scrape-off plasma is permeable to recycled Franck-Condon atoms. The ion flux to the walls is negligibly small compared with the flux to the divertor chambers, which is typical of a device with a large separatrix to wall distance. This means that practically the total recycling flux comes from the divertor chambers. The dominant cooling mechanism in the scrape-off zone is parallel electron heat conduction. As the equipartition time in the edge plasma is small compared with $\tau_\parallel = L/v_\Gamma$ (L length of field line), there exists close coupling between T_e and T_i.

1. INTRODUCTION

The development of transport codes including the boundary of tokamaks is important for understanding the processes in the scrape-off region and for designing advanced tokamak devices. At present, there is a considerable need for testing these codes against experimental findings in the boundary region of limiter and divertor tokamaks.

In this paper we deal with a computer model which attempts to take into account phenomenologically the essential physics in the scrape-off region and compare the results with ohmically heated divertor discharges in ASDEX /1/. A clear distinction between the scrape-off plasma treated here and the divertor chamber plasma is necessary since different processes are dominant in the two regions owing to large changes in parameters, e.g. smaller temperatures and orders of magnitude larger neutral hydrogen density in the divertor chamber. The simulations are carried out with a new version of the BALDUR transport code /2, 3/, called BALDIO8R, which incorporates a self-consistent 1-D scrape-off region model and a fast version of the AURORA Monte-Carlo neutral transport coding. A description of the modelling and the code is given in Section 2.

In Section 3 the results of the computer simulations are compared with ohmically heated DP discharges (divertor with pumping) in ASDEX and discussed in detail.

2. MODELLING AND CODE

At first we outline the processes taken into account in the improved version of the scrape-off model implemented in the BALDUR code. In keeping with experimental results for the edge plasma we assume anomalous cross-field diffusion and electron heat conduction in the scrape-off zone. The edge plasma of ASDEX is collision dominated. Convective particle (nv_Γ) and energy losses $||\vec{B}$ are simulated by a subsonic flow velocity v_Γ (= 1/7 v_s) with the local isothermal sound speed for 1-D flow $v_s = (\frac{kT_e+kT_i}{m_i})^{1/2}$.

Such a small value for v_Γ is derived from experiments on ASDEX. The use of such a model is supported by investigations of the end-losses from linear Θ-pinches /4/, which have shown that the temperature dependence of the ion sound speed model holds both in the collisionless and in the collisional regime.

There is experimental evidence in ASDEX that there exist temperature gradients $||\vec{B}$ between the divertor chamber and the scrape-off plasma in the torus. Moreover, the energy transported to the divertor room is partially delivered to the plasma and neutral gas there and lost by volume processes (charge exchange and radiation) and is partially deposited on the neutralizer plates /5/. The fraction of power lost before reaching the plates grows with increasing density. These observations suggest a separate treatment of the parallel losses due to heat conduction and convection.

In typical ASDEX discharges $\lambda_{ee}|\nabla_{\shortparallel} T_e| << T_e$, where λ_{ee} is the mean free path for electron-electron collisions, is satisfied all over the scrape-off zone so that $\vec{q}_{\shortparallel} = -\chi_{e\shortparallel}\nabla_{\shortparallel}(kT_e)$ may be applied. If one assumes div $\vec{q}_{\shortparallel} = 0$ between the scrape-off plasma in the torus and the sink of the heat flow in the divertor chamber, an analytic integration of the heat conduction equation with a classical $\chi_{e\parallel}$ yields $q_\parallel(r) \sim T_e(r)^{7/2}$, where T_e is evaluated in the scrape-off zone in the main chamber and $T_{e,sink} \ll T_e^{7/2}$ has been used. The contribution from $q_\parallel$ has been included in the energy equation of the electrons.

In addition, the model takes into account convective energy losses $\parallel \vec{B}$ by nv_Γ $(\frac{3}{2}\, kT_e + \frac{3}{2}\, kT_i)$ with the temperatures in the scrape-off zone of the main chamber. Further improvements of the code include a new "vectorized" version of the AURORA Monte-Carlo code which increases the speed of the calculation of neutral gas transport on the Cray-1 computer. Moreover, a numerical feedback control of gas puffing for density programming and a wide variety of transport models for the bulk and the scrape-off plasma are available to allow flexibility in fitting experimental data.

The transport coefficients for cross-field heat conduction and diffusion in the different radial zones that yielded best fits with the experiments are:

$\chi_{i\perp}$ 1x neoclassical

	$\chi_1 = 1.5\, D_B f_q$	$q \leq 1$
$\chi_{e\perp} =$	$\chi_2 = 2.7 \times 10^{17}\, n_e^{-1}\, T_{e,keV}^{-1/2}$	$q>1,\ r \leq 30$ cm
$(cm^2 s^{-1})$	$\chi_3 = \chi_2(30) + 0.1(r-30)(\chi_4 - \chi_2(30))$	30 cm $\leq r \leq$ 40 cm
	$\chi_4 = 2 \times 10^4$	$r \geq 40$ cm
	$D_1 = 0.1\, \chi_{e\perp}$	$q \leq 1$
$D_\perp =$	$D_2 = 0.1\, \chi_{e\perp}$	$q>1,\ r \leq 30$ cm
$(cm^2 s^{-1})$	$D_3 = D_2(30) + 0.1(r-30)(D_4 - D_2(30))$	30 cm $\leq r \leq$ 40 cm
	$D_4 = 1.6 \times 10^3$	$r \geq 40$ cm

Here D_B is the coefficient for Bohm diffusion and f_q is a function of q /2/. In the simulations 1 x neoclassical Ware pinch /2/ was used. As can be seen constant values of $\chi_{e\perp}$ and $D_\perp$ all over the scrape-off region (40 cm<r<49 cm) have been found sufficient to explain the measurements. For radially varying diffusivities more experimental input is needed. Sources and sinks of particles and energy include ionization and charge exchange, scrape-off losses, ohmic heating, line radiation and bremsstrahlung (Z_{eff} = 1.2 for gettered discharges). Gas puff neutrals and recycled neutrals are launched with 3.3 eV (Franck-Condon atoms). Backscattering from the walls is allowed in the Monte-Carlo computation of neutral hydrogen trajectories.

3. <u>COMPARISON WITH ASDEX</u>

The code has been used to simulate ohmically heated low density q = 4.4 (B_t = 22 kG, I_p = 246 kA) ASDEX discharges of type DP (divertor with pumping). Because of the very low impurity level with this mode of operation the impurity radiation in the torus may be neglected.

We begin with a discussion of a series of computer experiments by which the influence of $D_\perp$ and $\chi_{e\perp}$ in the scrape-off zone on the profiles of n, T_e and T_i was studied. The results are compared with analytical predictions and are used to determine the transport coefficients in the scrape-off region from measured scrape-off scale heights. Then we compare the results of the simulations of ASDEX discharges with the experimental findings. Finally, the particle and energy balances and the influence of parallel heat conduction on the scrape-off losses and temperature profiles are discussed.

Like the analytic steady-state solutions for the scrape-off region /3/ the computed n, T_e, T_i and the particle flux $||\vec{B}$ decay $\sim \exp(-\frac{r-r_{sep}}{\lambda})$ over a substantial fraction of the scrape-off zone, where r_{sep} is the separatrix radius (40 cm) and λ is the corresponding scrape-off length. Variation of the diffusion coefficient $D_\perp$ (see Fig. 1) shows that the density scrape-off length scales approximately like $\lambda_n = (D_\perp \frac{\tau_i \tau_\parallel}{\tau_i - \tau_\parallel})^{1/2}$, where $\tau_i = (n_o < \sigma_i v_e >)^{-1}$ and $\tau_\parallel = L/v_\Gamma$ (L length of magnetic field line). In Fig. 1 $\lambda_n = (D_\perp \tau_\parallel)^{1/2}$, which does not include ionization ($\tau_i \rightarrow \infty$), is also given for comparison.

In the low density ASDEX discharges studied here only little ionization of Franck-Condon neutrals by the scrape-off plasma takes place as is demonstrated by the flat n_o profile in Fig. 5, which is characteristic of permeable plasmas. This means that the recycling neutrals practically cannot affect λ_n by becoming ionized in the scrape-off plasma and makes λ_n independent of the recycling coefficient ρ in the simulations. ρ is defined as the flux of recycled atoms divided by the ion flux to the torus wall or through the divertor throat.

The solid curves in Fig. 2a show the evolution of toroidal plasma current I_p and line averaged electron density $\bar{n}_e$ for the investigated DP discharges. The circles represent the simulated $\bar{n}_e$ program achieved by numerical feedback control of gas puffing. The decay of $\bar{n}_e$, after closing the gas puff valve at 1.71 s, to the prescribed value of 2.6×10^{12} cm^{-3} is used to determine the recycling coefficient ρ by a trial and error procedure. A best fit to the $\bar{n}_e$ decay in Fig. 2a is obtained with $\rho = 0.2$, which is kept constant during the whole discharge. In Figs. 2b and 2c measured (circles) and simulated profiles (solid curves) with the transport coefficients listed in Section 2 are compared at 0.5 and 1.0 s.

Especially at t = 1 s the agreement is satisfactory if one takes into account the experimental error. The computed density profiles show large shoulders at $r \gtrsim 30$ cm that disagree with the measurements and might be ascribed to an inadequacy of the empirical transport laws probably in the bulk plasma. A flow velocity $v_\Gamma = 1/7\ v_s$, $D_\perp = 1.6 \times 10^3\ cm^2\ s^{-1}$ ($\lambda_n = 1.5$ cm) and $\rho = 0.2$ are consistent parameters. The computed gas puff rate is influenced by nv_Γ and ρ. It amounts to 1.8×10^{21} atoms s^{-1} and is also consistent with the experiments, if one takes into account that only a fraction of the hydrogen molecules puffed in is dissociated before becoming ionized or adsorbed on the walls and contributes to the influx of Franck-Condon neutrals. The simulations show that the ion flux on the torus wall is negligibly small compared with the ion flux through the divertor throats. Such a situation is typical of devices with a large distance between separatrix and wall. Consequently, the recycling of neutrals essentially occurs from the divertor chambers.

At t = 1 s the simulation yields a total energy confinement time (thermal energy/ohmic power) of 41 ms which agrees with the experimental value. The computations show that at t = 1 s the total ohmic heating power is 329 kW while the losses in the main chamber due to charge exchange and radiation (hydrogen line radiation and bremsstrahlung) amount to 31.5 kW and 11 kW, respectively. Heat conduction and convection losses $\perp \vec{B}$ to the walls are 0.3 kW and are thus negligibly small. The residual heating power equals the scrape-off losses due to parallel heat conduction (261 kW, 91 %) and due to convection $\|\vec{B}$ (25.5 kW, 9 %). The dominant cooling mechanism in the scrape-off zone is thus parallel electron heat conduction.

In Fig. 3 the corresponding computed T_e profile (solid curve) in the scrape-off zone is shown, which roughly agrees with first results of T_e measurements in this region by Thomson scattering. The dashed curve was obtained by a different scrape-off model that does not separately treat the losses due to heat conduction and convection along the magnetic field /3/. This model assumes an infinite $\chi_{e\parallel}$ and $\nabla_\parallel T_e = 0$ and describes the combined parallel heat conduction and convection losses by the energy flux $nv_\Gamma(2\gamma_e kT_e+2kT_i)$ through the sheath potential in front of the neutralizer plates. In ASDEX secondary electron emission may be neglected ($\gamma_e = 2.9$) because the magnetic field lines graze the neutralizer plates and thus force the secondary electrons back. The $\chi_{e\perp}$ value corresponding to the solid curve in Fig. 3 (2×10^4 cm^2 s^{-1}) was determined from a parametric scan studying the variation of the temperature scale heights λ_{Te} and λ_{Ti} with $\chi_{e\perp}$ (see Fig. 4). An essentially linear increase with $\chi_{e\perp}$ was found. Since the equipartition time (0.3 ms) is short compared with $\tau_\parallel$ ($\approx$ 1.5 ms), rather close coupling between λ_{T_i} and λ_{T_e} results. This behaviour is also demonstrated by computed temperature profiles in the scrape-off region shown in Fig. 5. Since parallel heat conduction primarily affects the electrons, T_e values are everywhere smaller than T_i. The density profile n_o of neutral hydrogen (see Fig. 5) is remarkably flat over the scrape-off region, which is characteristic of plasmas permeable to neutrals. Obviously, a small ionization only occurs near the separatrix.

4. CONCLUSIONS

Comparisons with experimental data show that the transport processes in the scrape-off region of ohmically heated DP discharges of ASDEX can be adequately simulated by a 1-D self-consistent scrape-off model in the BALDUR transport code which uses a fluid description of the plasma and a

Monte-Carlo modelling of neutrals. The scrape-off model is phenomenological in the sense that cross-field diffusion $D_\perp$, electron heat conduction $\chi_{e\perp}$, parallel flow velocity and recycling coefficient must be fitted to the experiments. Anomalously high $D_\perp$ and $\chi_{e\perp}$ values are obtained in the scrape-off zone which do not differ much from the transport coefficients of the bulk plasma. This suggests that no abrupt changes in cross-field transport laws seem to be required for the scrape-off region.

Moreover, the numerical simulations demonstrate that in the discharges studied here ASDEX behaves like a device with a large separatrix to wall distance. The negligibly small ion flux $\perp \vec{B}$ on the torus walls compared with the flux $||\vec{B}$ suggests that neutrals recycle mainly from the divertor chambers. Owing to its small line density the scrape-off plasma becomes permeable to Franck-Condon atoms. This explains the result of the simulations that the recycling flux of neutrals enters the total particle balance but does not influence the scrape-off scale heights.

From the detailed energy balance one can conclude that almost all of the ohmic heating power is lost in the scrape-off zone by transport processes parallel to the magnetic field. In the investigated small density discharges without an edge cooling due to impurities and with electron temperatures of about 40 eV near the separatrix the power loss due to convection $||\vec{B}$ is far outdone by the loss due to parallel electron heat conduction. Since the scrape-off plasma of ASDEX is collision dominated, a close coupling of electron and ion temperatures occurs. The strong T_e dependence ($\sim T_e^{7/2}$) of the energy flow due to parallel heat conduction produces rather small temperature scrape-off scale heights. Moreover, it causes a sensitive scaling of the ratio of the conductive and convective losses with the T_e values near the separatrix.

ACKNOWLEDGEMENTS

The authors acknowledge the support of following people: The ASDEX team for experimental data, the BALDUR group for their transport code, J. Ogden, D. Post and R. Jensen for a version of the scrape-off model, A. McKenney for the vectorized version of AURORA, F. Seidl, A. Silverman and R. Wunderlich for computational support and K. Lackner for discussions.

REFERENCES

/1/ Keilhacker, M. et al., Proc. 8th Conf. Plasma Phys. and Contr. Nucl. Fus. Res. 1980, Vol. II, 351

/2/ Post, D.E., Singer, C.E., McKenney, A.M. and PPPL Transport Group, TFTR Physics Group Report 33 (1981)

/3/ Ogden, J.M., Post, D.E., Jensen, R.V. and Seidl, F.G.P., PPPL-1608 (1980)

/4/ McKenna, K.F. et al., Proc. 7th Conf. Plasma Phys. and Contr. Nucl.Fus.Res. 1978, Vol. II, 229

/5/ Müller, E.R., Niedermeyer, H., Report IPP III/74 (1981)

FIGURE CAPTIONS

Fig. 1 Density scrape-off length λ_n vs. $D_\perp$ compared with analytic relations.

Fig. 2 Simulated ASDEX DP discharges ($q = 4.4$)

a) programs of I_p and line averaged density $\bar{n}_e$ in experiment (solid curves) and computation (circles),

b) and c) experimental (circles) and code results (solid curves) for t = 0.5 and 1.0 s.

Fig. 3 Computed T_e profiles in the scrape-off region with convection and heat conduction $||\vec{B}$ compared with T_e measurements: Present model (solid curve), model with infinite $\chi_{e\parallel}$, $\nabla_\parallel T_e = 0$ (dashed curve).

Fig. 4 Temperature scrape-off lengths λ_{Te} and λ_{Ti} vs. $\chi_{e\perp}$ with convection and heat conduction $||\vec{B}$.

Fig. 5 Detailed plots of computed density and temperature profiles in the scrape-off zone.

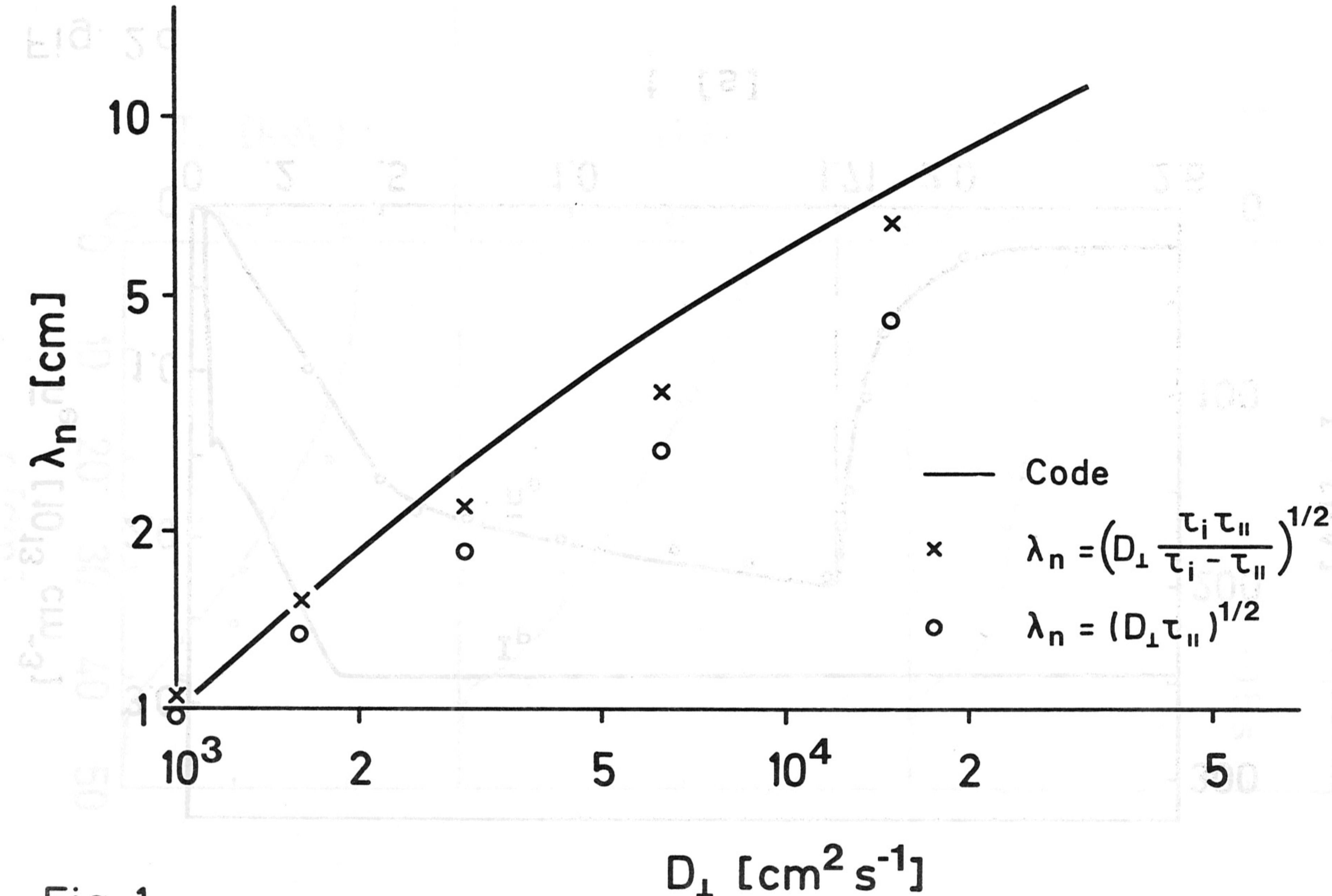

10
5
2
1
λ_n [cm]
10^3
2
5
10^4
2
5
$D_\perp$ [$cm^2 s^{-1}$]
Code
$\lambda_n = \left(D_\perp \frac{\tau_i \tau_\parallel}{\tau_i - \tau_\parallel}\right)^{1/2}$
$\lambda_n = (D_\perp \tau_\parallel)^{1/2}$

Fig. 1

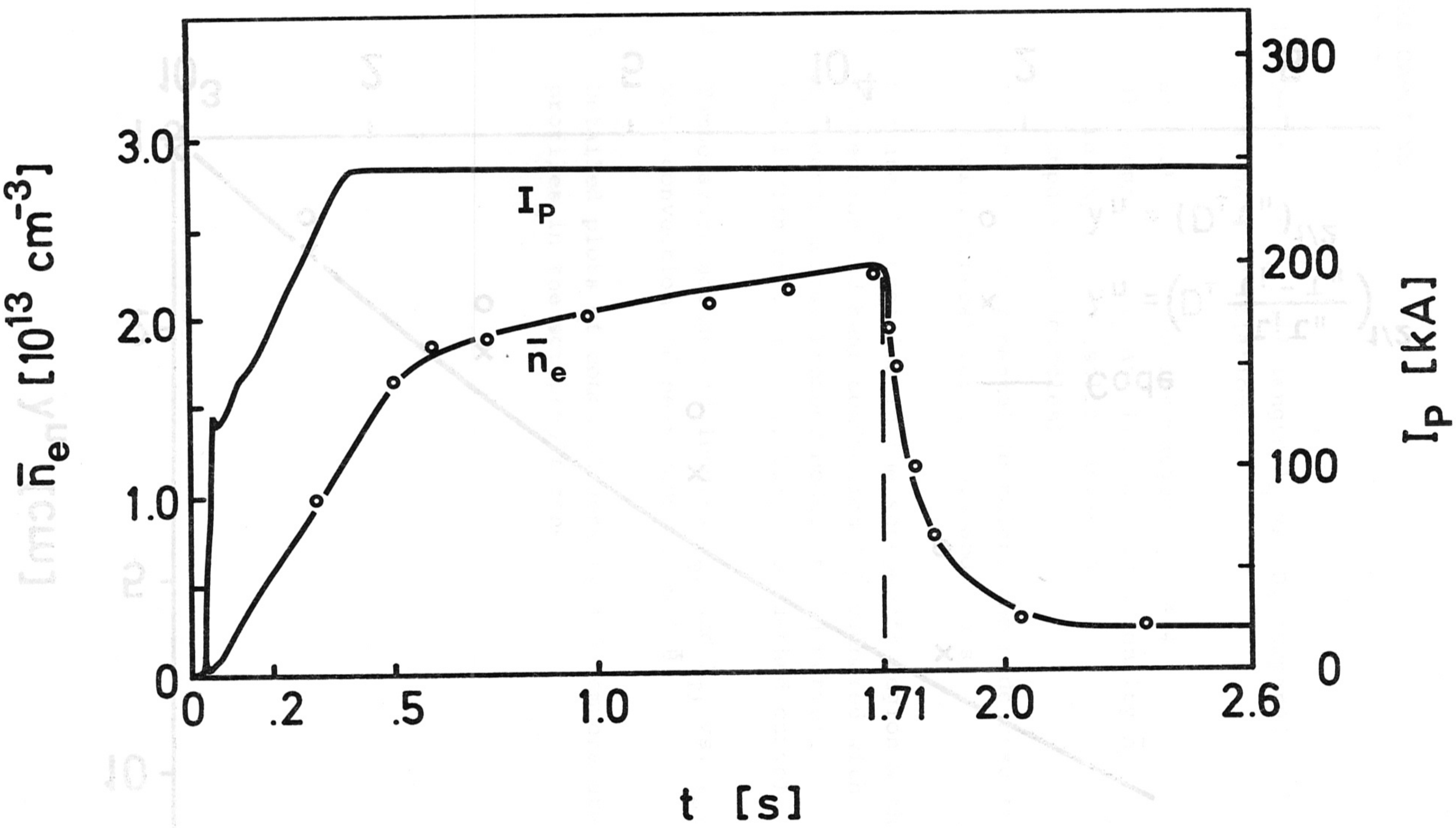

$\bar{n}_e$ [10^{13} cm^{-3}]
3.0
2.0
1.0
0
I_P [kA]
300
200
100
0
I_P
$\bar{n}_e$
0
.2
.5
1.0
1.71
2.0
2.6
t [s]

Fig. 2a

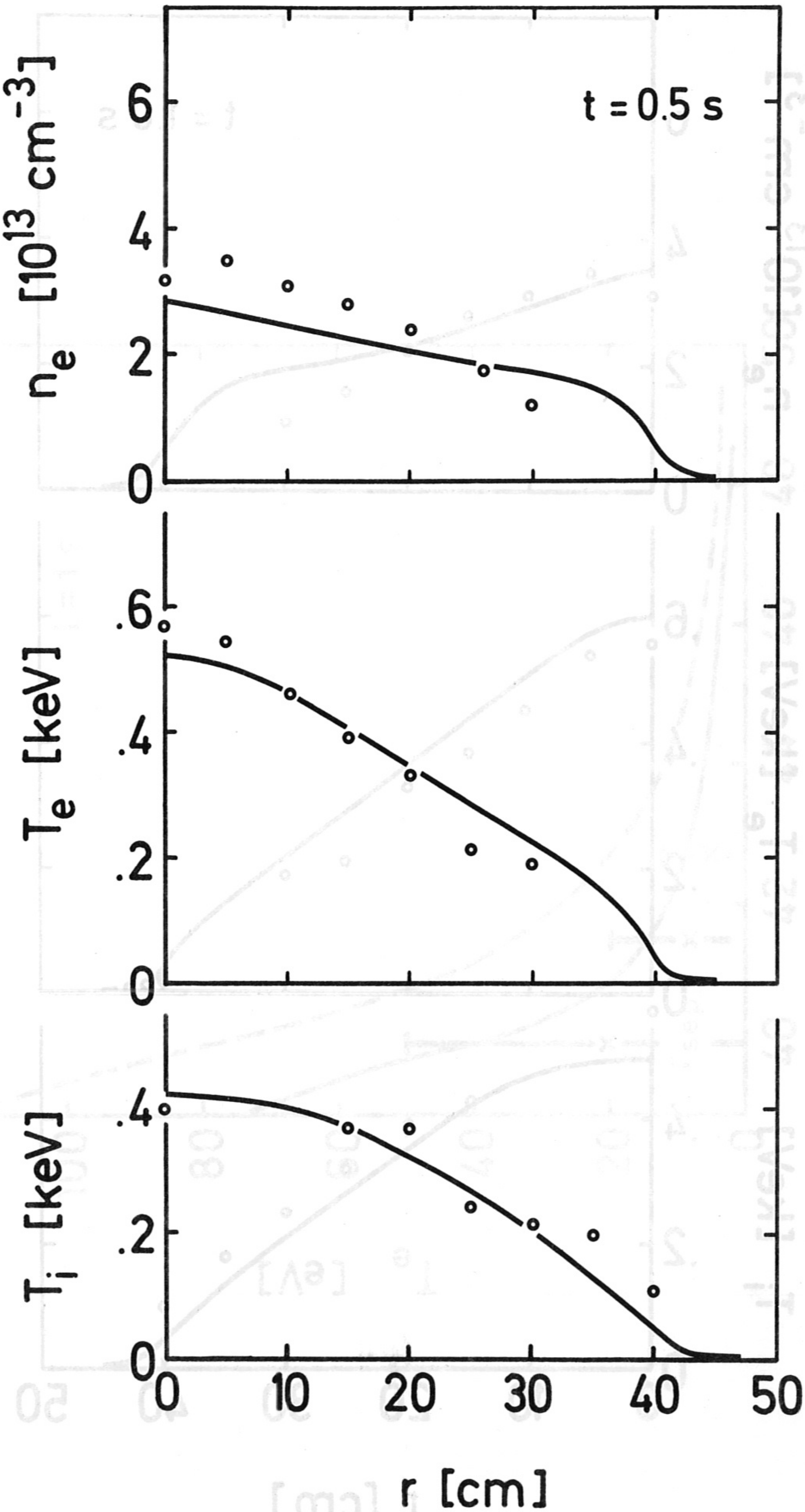

Fig. 2 b

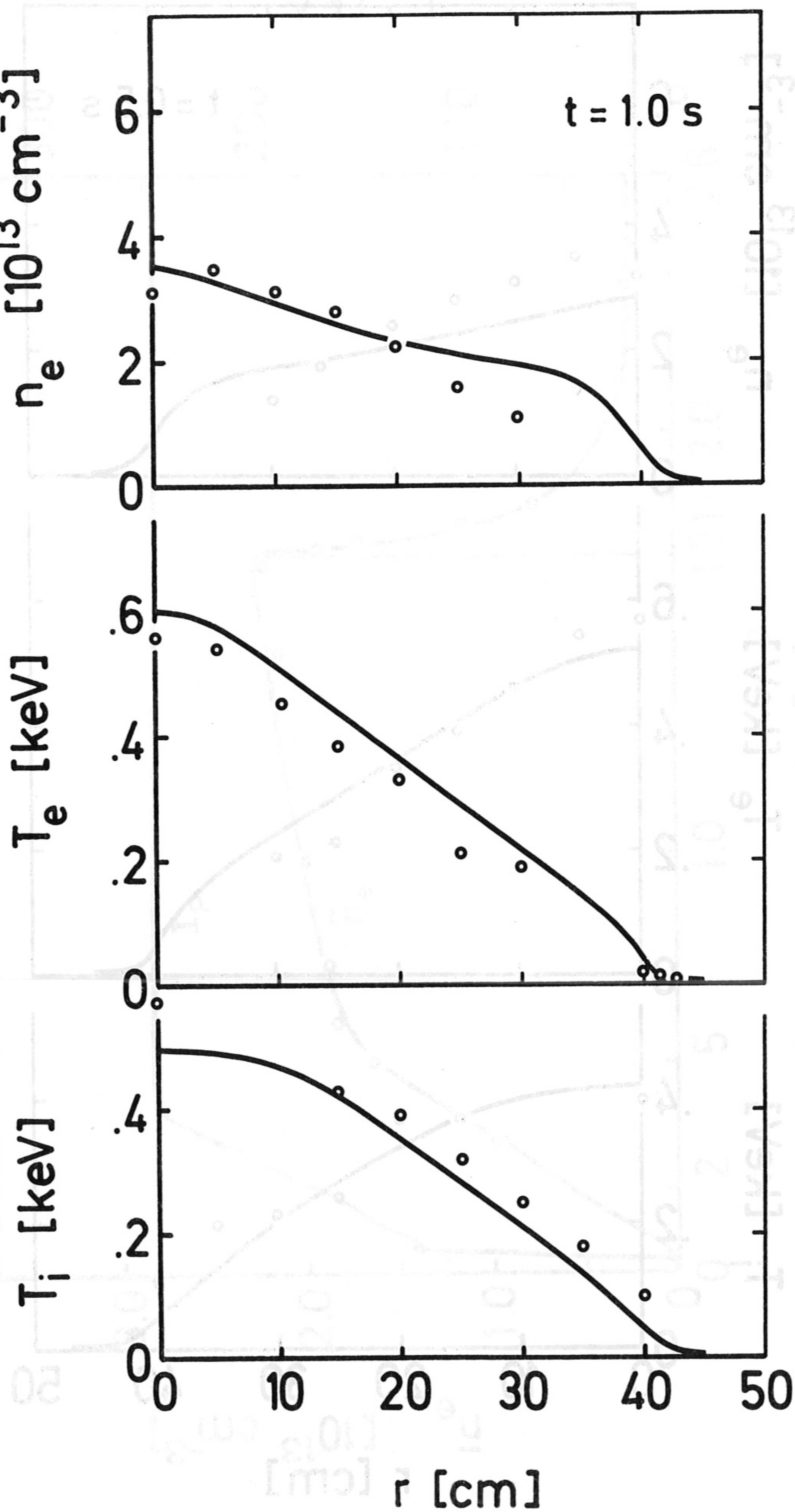

Fig. 2c

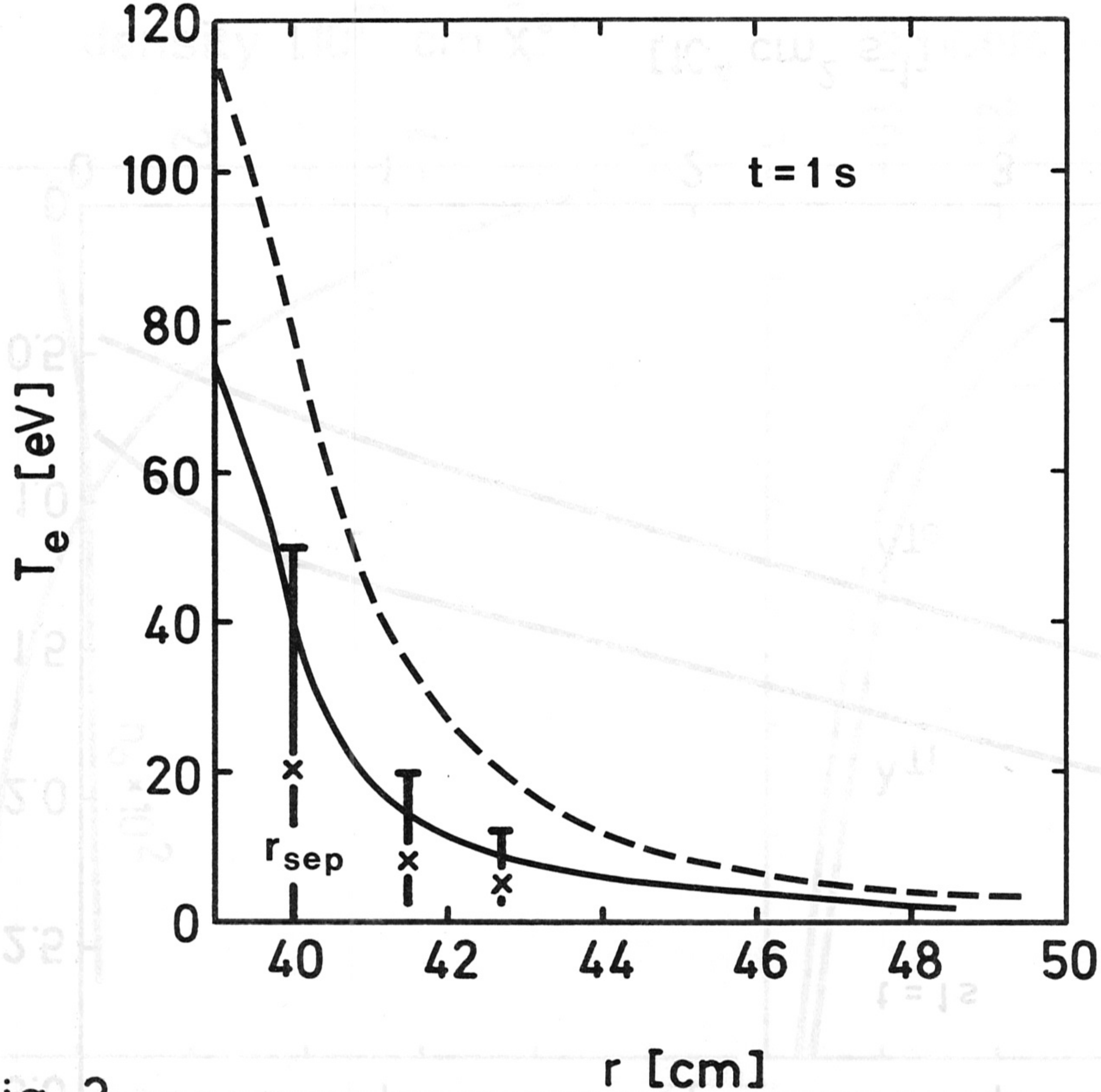

Fig. 3

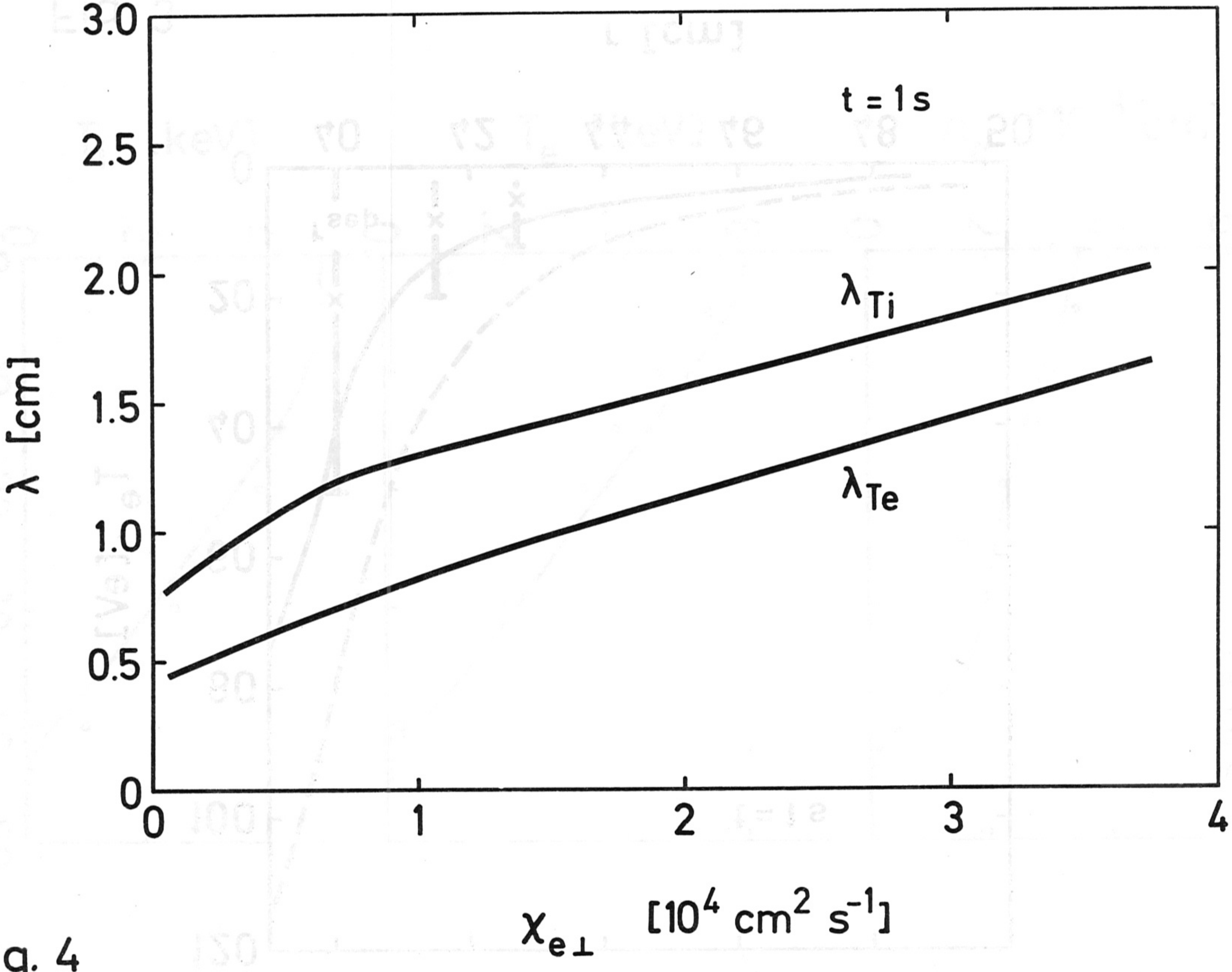

Fig. 4

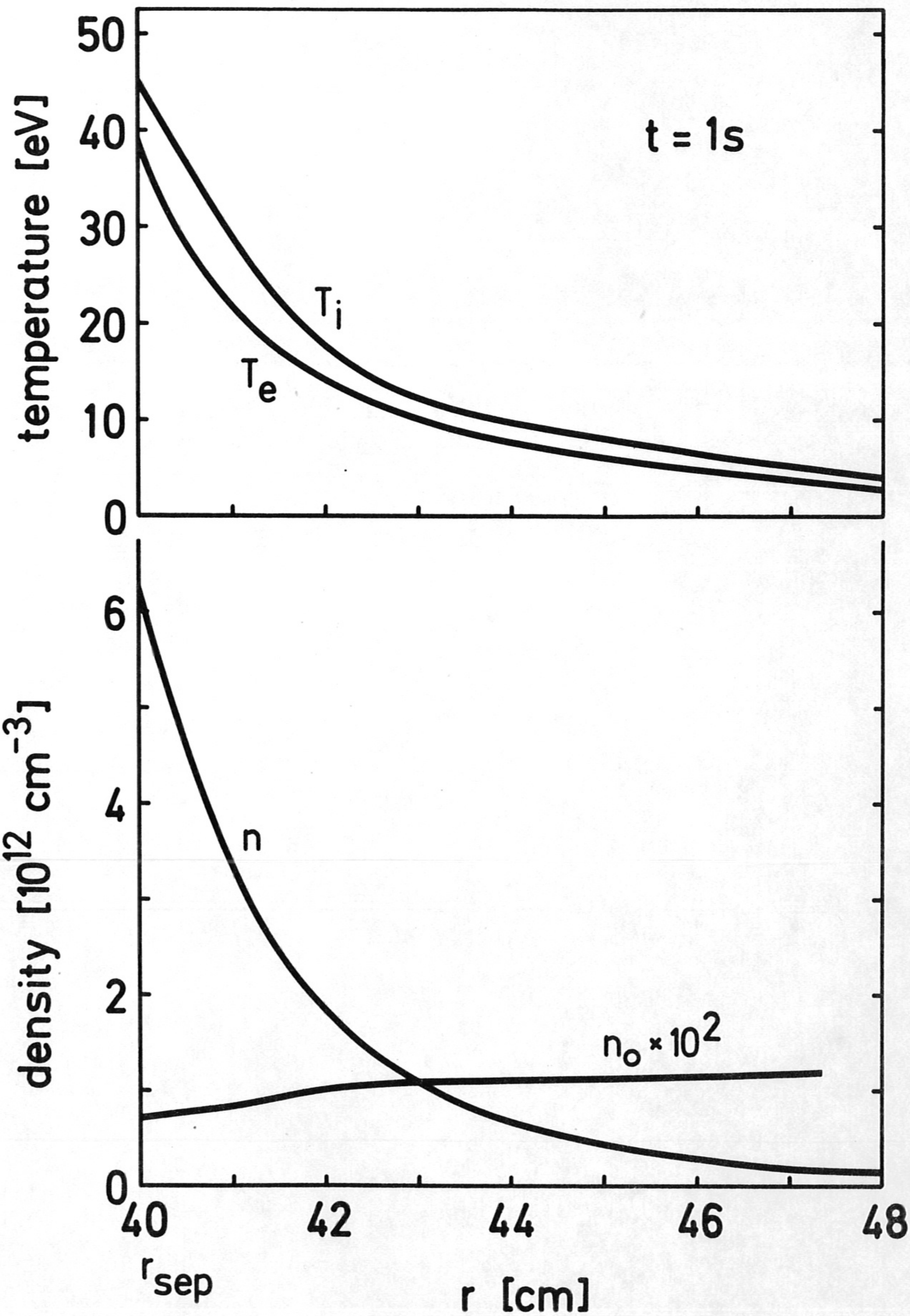

50
40
30
20
10
0
temperature [eV]
t = 1s
T_i
T_e
6
4
2
0
density [10^{12} cm^{-3}]
n
$n_o \times 10^2$
40
42
44
46
48
r_{sep}
r [cm]

Fig. 5